

Devoid Clutter Capture and Filling (DeCCaF) to Compensate for Intra-CPI Spectral Notch Variation

Jonathan W. Owen, Brandon Ravenscroft, Shannon D. Blunt
Radar Systems Lab (RSL), University of Kansas
Lawrence, KS, USA

Abstract—Cognitive spectral notching of FM noise waveforms on transmit has been experimentally shown to be an effective means with which to avoid in-band interference. However, to contend with dynamic interference the transmit notch may be required to move during the coherent processing interval (CPI), which introduces a nonstationarity effect that results in increased residual clutter after cancellation. It was recently shown that optimal mismatched filtering (MMF) can partially mitigate this degradation while maintaining the necessary spectral notch for interference mitigation.

Here a new approach to compensate for this nonstationarity is proposed that borrows the missing portion of the clutter (due to notching) from another pulsed response for which the notch is in a different location. By using this borrowed response to fill in the notched clutter, subsequent clutter cancellation largely avoids the nonstationarity effect so that the corresponding residue is reduced. It is shown using measured data that the combination of this clutter filling approach with notched MMFs realizes clutter cancellation performance on par with full-band random waveforms that do not possess spectral notching.

Keywords—spectrum sharing, cognitive radar, spectrum notching, clutter cancellation, FM noise waveforms

I. INTRODUCTION

Increased competition for RF spectrum, particularly for the large swaths occupied by radar [1], is motivating research into spectrum sharing (e.g. [2-4]) as well as some forms of cognitive radar (e.g. [5-10]) that are able to sense and avoid radio frequency interference (RFI). When RFI is dynamically changing during the coherent processing interval (CPI) of the radar this interference avoidance capability must likewise perform at or near the rate of the pulse repetition frequency.

It was recently shown that a rapid band-aggregation method [9], coupled with the ability to design and physically generate spectrally notched radar waveforms [11] possessing an FM noise structure [12], provides a prospective solution to the problem of dynamic RFI. The FM nature of these waveforms makes them appropriate for high-power radar applications, which represent the situations whereby one would expect the greatest amount of interference to be produced by the radar to other spectrum users.

It has been experimentally shown that spectral notches having better than 50 dB depth relative to the peak of the power spectrum can be achieved for modest transmitter distortion [11, 13]. Similar interference rejection can subsequently be obtained within the radar receiver during pulse compression simply by performing matched filtering, under the caveat that the receiver is not saturated [14].

However, a notable limitation that has been observed, even when spectral notches are able to precisely track the spectral locations of in-band RFI, is that changing notch locations during the CPI introduces a nonstationarity effect that hinders clutter cancellation [11]. It has been shown that this degradation is linked to a distortion of the delay/Doppler point spread function [11].

It has very recently been demonstrated [15] that the use of a spectrally notched form of optimal mismatched filtering (MMF) via [16] can partially compensate for this degradation. Generally speaking, the MMF approach addresses the range sidelobe modulation (RSM) of clutter that naturally arises when varying the waveform during the CPI [12, 17-20].

The nonstationarity induced by changing notch locations is more than a clutter RSM effect, however, and thus further steps are required to compensate for the remaining residual clutter. To that end, an ad hoc approach denoted as devoid clutter capture and filling (DeCCaF) is proposed whereby the clutter response from a different pulse is bandpass filtered (BPF) commensurate with the notch location in the present pulse, and then subsequently added to the clutter response for the present pulse. Measured data collected using waveforms having moving spectral notches is used to assess the efficacy of this approach.

II. COGNITIVE SPECTRAL NOTCHING

The approach described and experimentally evaluated in [11] performs sensing of the spectrum at each pulse repetition interval (PRI) to ascertain the presence/location(s) of in-band RFI. The fast spectrum sensing (FSS) method developed in [9] that was inspired by the human thalamus applies an efficient process to determine the portions of the band within which the radar could reasonably operate (i.e. discern the regions having sufficient uninterrupted swaths of spectrum that do not contain other users). This information informs subsequent FM noise waveform design with regard to the spectral locations where notches are required.

Being FM, these waveforms are continuous and possess adequate spectral containment (i.e. good roll-off) to make them amenable to a high-power transmitter. They are designed using discretized versions that are sufficiently over-sampled with respect to 3-dB bandwidth such that unavoidable aliasing (for a time-limited pulse) is minimized according to the degree of fidelity required. The approaches in [11] and [13] represent two distinct ways in which notched FM noise waveforms could be obtained.

The baseline receive processing of the resulting radar responses is then rather standard. The incident reflections are matched filtered, where the transmit spectral notch(es) likewise serves to suppress the in-band RFI (assuming the receiver is not saturated [14]). Subsequent Doppler processing and clutter cancellation (if needed) are likewise standard.

However, the waveform agility that provides the design freedom needed to perform this manner of cognitive spectral notching does experience clutter range sidelobe modulation (RSM) due to the pulse-to-pulse changing sidelobe structure. As such, subsequent clutter cancellation produces a residue that necessitates further consideration to address.

The earlier approaches to compensate for RSM [17, 19] sought to make the filtered responses of different waveforms be as similar as possible (i.e. decrease the pulse-to-pulse variation of sidelobes), though doing so often tended to

increase the sidelobe level. In contrast, MMF-based approaches [12, 18] tend to be easier to implement and result in better overall RSM mitigation by simply reducing the sidelobes experienced by each pulse (or subset of pulses [20]).

Importantly, the MMFs in this waveform agility context are based on the FM version of the Least-Squares (LS) MMF described in [16], in which a form of “beamspoiling” is employed to avoid the degradation from super-resolution that otherwise occurs due to the over-sampling necessary for high fidelity. Moreover, for application to cognitive RFI avoidance, each unique MMF must also contain spectral notching that aligns with the given notched waveform as considered in [15]. Care must be taken so that the inverse nature of the LS MMF does not invert the desired spectral notch (otherwise causing RFI enhancement [21]), but instead preserves good notch depth for interference suppression on receive as well.

In addition to the RSM produced by waveform agility, it has been observed that moving spectral notches during the CPI also has an impact on the pulse compression mainlobe. Consequently, while the MMF approach is still certainly beneficial, it alone does not fully address the residual clutter issue in this case [15]. To that end, we propose the DeCCaF approach, which will be applied using both matched filtering and MMF for comparison.

III. LS-MMF FOR NOTCHED FM NOISE WAVEFORMS

As a quick review, denote the radar waveform as $s(t)$. It has pulse width T and 3-dB bandwidth B . Let K indicate the amount of over-sampling with respect to 3-dB bandwidth to achieve sufficient fidelity. Denote this discretized version as $\mathbf{s} = [s_1 \ s_2 \ \dots \ s_N]^T$, where $N = K(BT)$ is the length of vector \mathbf{s} .

Per [16], construct the banded Toeplitz matrix

$$\mathbf{A} = \begin{bmatrix} s_1 & 0 & \cdots & 0 \\ \vdots & s_1 & \ddots & \vdots \\ s_N & \vdots & \ddots & 0 \\ 0 & s_N & & s_1 \\ \vdots & & \ddots & \vdots \\ 0 & \cdots & 0 & s_N \end{bmatrix}, \quad (1)$$

which has dimensions $((M+1)N - 1) \times MN$, for MN the length of the MMF (2N to 4N typically). The MMF filter is then [16]

$$\mathbf{h}_{\text{MMF}} = (\tilde{\mathbf{A}}^H \tilde{\mathbf{A}} + \sigma \mathbf{I})^{-1} (\tilde{\mathbf{A}}^H \mathbf{e}_m), \quad (2)$$

where σ is a diagonal loading factor, \mathbf{I} is an $MN \times MN$ identity matrix, \mathbf{e}_m is a length $((M+1)N - 1)$ elementary vector with a ‘1’ in the m th position (usually near the middle) and zeros elsewhere, and $(\bullet)^H$ is the Hermitian operator.

An important distinction is that the matrix $\tilde{\mathbf{A}}$ in (2) is the same as \mathbf{A} defined in (1) but with the $K - 1$ rows above and below the m th row replaced with zeros. This modification provides the “beamspoiling” needed to avoid degradation caused by super-resolution due to \mathbf{s} being over-sampled. For all following results the value of σ is set to be 10% of the largest eigenvalue of $(\tilde{\mathbf{A}}^H \tilde{\mathbf{A}})$.

IV. DEVOID CLUTTER CAPTURE AND FILLING (DECCAF)

Moving spectral notches during the CPI (due to dynamic RFI) hinders clutter cancellation because the changing notch locations introduce a significant deviation from the average spectral density of the set of waveforms in the CPI. Modest

variation of the spectral density already occurs for notch-free random FM waveforms (even those obtained via spectral shaping), though the application of appropriate MMFs has been found to compensate to a sufficient degree [12, 18, 20]. The presence of moving notches, however, necessitates more substantial steps to “homogenize” the individual spectral densities.

Consider a set of M random FM waveforms denoted $s_m(t)$ for $m = 1, 2, \dots, M$ that possess the same general spectral density aside from *a*) modest variation due to their random nature and *b*) spectral notch locations that may change on a pulse-to-pulse basis. For ease of explanation we shall focus on the case in which only a single notch is present for each pulse, though the proposed compensation approach is readily extensible to multiple notches.

The reflected response after transmitting this sequence of waveforms can be expressed as

$$y_m(t) = s_m(t) * x_m(t) + v_m(t), \quad (3)$$

where $*$ is the convolution operation, $x_m(t)$ is the impulse response of the environment during the m th PRI, and $v_m(t)$ is additive noise. Internal clutter motion notwithstanding, one could generally expect the clutter component of this term to be essentially unchanged over the CPI.

Pulse compression of (3) is then performed via

$$z_m(t) = h_m(t) * y_m(t), \quad (4)$$

for $h_m(t)$ the matched filter (or MMF) of the m th waveform. Normally, Doppler processing and clutter cancellation would then be performed across the set of M responses from (4). However, when waveform spectral notches are present that move during the CPI a result like that depicted in Fig. 1 is obtained. These experimentally measured results were collected from a stationary platform observing moving vehicles leaving/entering an intersection in Lawrence, KS. Simple projection-based clutter cancellation was applied that has otherwise been found to be sufficient to the task when spectral notches are either absent or do not move during the CPI (see [11]). The residual clutter, which takes the form of the large streaks across Doppler in Fig. 1, is caused by the nonstationarity introduced by moving the spectral notches.

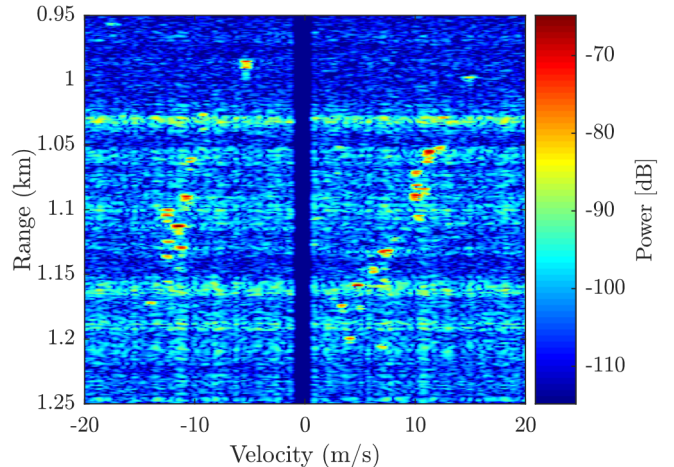


Fig. 1. Experimentally measured range-Doppler response to random FM waveforms with changing spectral notches (match filtered)

The DeCCaF approach seeks to compensate for this residual clutter effect via an ad hoc “clutter filling” solution. While the notion of estimation/interpolation of static spectral

notches is well-known for wideband radar applications to compensate/enhance image quality (e.g. [22, 23]), the distinction here is that we wish to mitigate clutter modulation so as to better facilitate clutter cancellation.

For DeCCaF, if the m th waveform contains a spectral notch at a given location, a similar spectral portion of the clutter is borrowed from the response generated by a different waveform that does not have a notch in that same location. Denoting the index of that other waveform as \tilde{m} and $w_m(t)$ as a bandpass filter (BPF) whose passband aligns with the notch location of the m th waveform, the borrowed clutter component is

$$c_{m,\tilde{m}}(t) = w_m(t) * z_{\tilde{m}}(t). \quad (5)$$

Thus the DeCCaF response is obtained by simply combining the original response with the borrowed clutter via

$$\bar{z}_m(t) = z_m(t) + c_{m,\tilde{m}}(t). \quad (6)$$

Subsequent clutter cancellation is then performed on the spectrally homogenized data from (6).

As an illustration of the concept, Fig. 2 depicts the loopback measured spectra for a full-band waveform (no notch), a notched waveform, and the BPF version of the full-band waveform corresponding to the notch. These full-band and notched waveforms were obtained from completely independent initializations and optimization processes, and thus the only thing they have in common is the same general spectrum shape. While this “quick and dirty” combination of the notched and BPF waveforms would not yield a spectrum that is identical to that of the full-band waveform, the result is rather close. Further, since convolution is a linear operation, consideration of Fig. 2 in the context of (3) and (6) implies that this approach should do a decent job of recapturing the missing clutter component as long as the clutter phenomenology is sufficiently stationary.

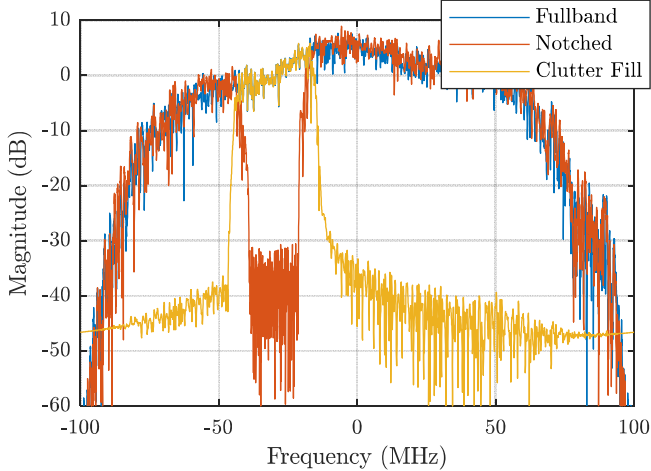


Fig. 2. Loopback measured spectra for a full-band (no notch) waveform, a notched waveform, and a BPF version of the full-band waveform

V. EXPERIMENTAL EVALUATION OF DECCAF

To establish a baseline for achievable performance using this clutter borrowing/filling approach, two sets of unique random waveforms were transmitted in an open-air setting with an interleaved arrangement (see Fig. 3). Both sets were generated according to the pseudo-random optimized (PRO) FM scheme developed in [12]. One set contains 2500 full-

band waveforms that are all independently initialized and optimized. The other set likewise contains 2500 independent waveforms, though for these a spectral notch moves to a new random location within the 3-dB bandwidth after every fourth pulse.

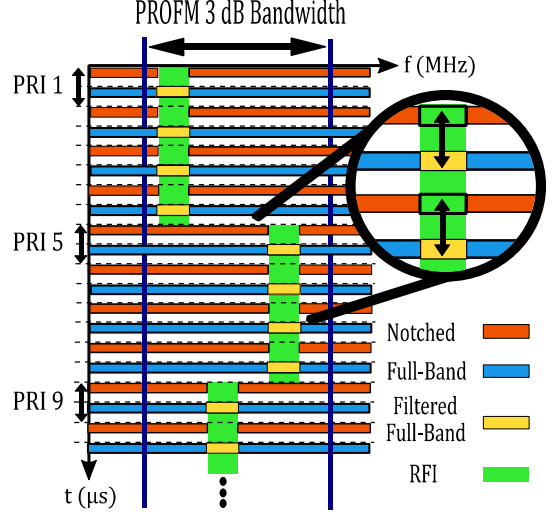


Fig. 3. Timing diagram of the waveform arrangement used for experimental evaluation of DeCCaF. Full-band and notched waveforms are interleaved, with the borrowed clutter taken from an adjacent full-band response.

This waveform arrangement is clearly not suitable for actual cognitive interference avoidance due to the presence of the interleaved full-band waveform but is used here to provide a controlled experiment regarding the utility of borrowed clutter responses. Consequently, four different cases are considered, all illuminating the same measured scene. These are 1) full-band random waveforms, 2) random waveforms with moving notches and no clutter filling, 3) random waveforms with moving notches where DeCCaF is applied using interleaved full-band responses to performing clutter filling, and 4) the full-band responses are disregarded and the borrowed clutter responses are taken from other notched waveform responses. The last of these represents the operating arrangement one would expect in practice. Both matched filtering and MMF via [15] are applied for each case.

It is important to note that, while the primary purpose of this manner of cognitive operation is to mitigate mutual RFI between the radar and other in-band spectrum users, the following results contain the associated spectral notches but not the RFI itself. In [11, 14] the degradation from RFI was shown to be significantly reduced, particularly when the RFI possesses good spectral containment. Consequently, here we focus solely on the limitation imposed by the moving spectral notches that provide this mutual RFI suppression.

For experimental measurements the PRI is 40 μs and is defined as the time between each interleaved pair of pulses. Each pulse has a duration of 2 μs and a 3-dB bandwidth of $B = 100$ MHz. Thus each waveform of either type has a time-bandwidth product of $BT = 200$. The CPI for each set of waveforms is 100 ms. The radar emissions were generated at a center frequency of 3.55 GHz, with the reflected echoes captured as I/Q data at a rate of 200 Msamples/s.

Each spectral notch has a bandwidth of $B/10$, with the locations randomly assigned within B . Spectral shaping of each notch edge via a Tukey taper was also employed to reduce $\sin(x)/x$ range sidelobes that otherwise occur [11].

Free-space measurements were collected using separate, yet collocated, transmit and receive antennas on the roof of Nichols Hall on the University of Kansas campus. The waveforms were produced by a Tektronix AWG70002a arbitrary waveform generator and the resulting responses captured with a Rohde & Schwarz FSW26 real-time spectrum analyzer. The illuminated scene was the intersection of 23rd and Iowa Streets in Lawrence, KS. A loopback measurement of each waveform was also collected so that each matched filter (MF) and MMF could account for the distortion introduced by the transmitter.

Clutter cancellation was applied to the set of reflected responses in each of the three cases by performing a simple zero-Doppler projection (since the platform is stationary) and with the inclusion of a Taylor window to reduce Doppler sidelobes. The LS FM-based MMF was constructed according to [15] with a length that is 3× that of the MF and with diagonal loading to avoid notch inversion.

A. Full-band random FM waveforms (baseline)

Figures 4 and 5 show the measured range-Doppler responses from the set of full-band PRO-FM waveforms (Case 1) after applying the MF and the MMF from [16]. While the MMF exhibits a noticeable reduction in the background noise, which for the most part is actually RSM being suppressed, both figures possess clearly identifiable moving targets. These results are provided to establish a performance baseline for notching and subsequent compensation.

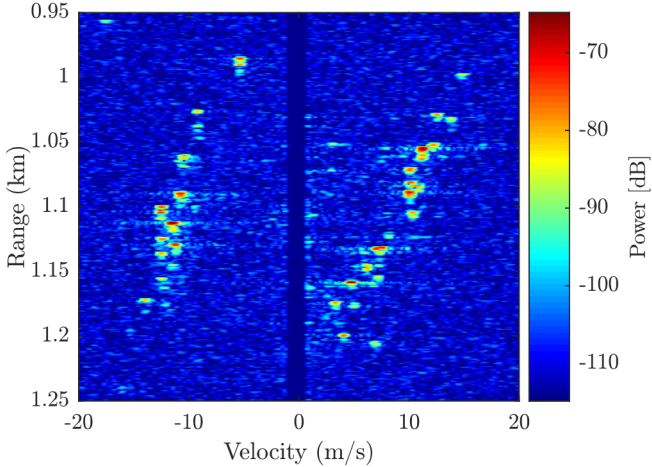


Fig. 4. Measured range-Doppler response from 2500 full-band PRO-FM waveforms (using MF)

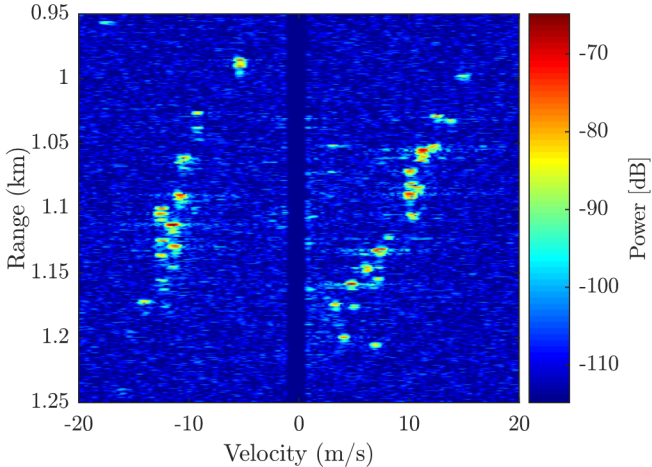


Fig. 5. Measured range-Doppler response from 2500 full-band PRO-FM waveforms (using MMF)

B. Random notched FM waveforms

Figure 6 (repeated from Fig. 1) and Fig. 7 illustrate the degradation that arises for MF and MMF (via [15]), respectively, when notched PRO-FM waveforms are employed and the notch locations move during the CPI (Case 2). The streaks observed in Fig. 6 are smeared clutter that could not be cancelled due to the nonstationarity induced by changing notch locations. The use of notched MMFs in Fig. 7 does provide some compensation for this effect, but it does not completely mitigate the degradation. As discussed above, the reason is that the MMFs are addressing the RSM issue, which certainly helps, but not the more significant nonstationarity introduced by the moving notches. These results are consistent with those obtained in [15].

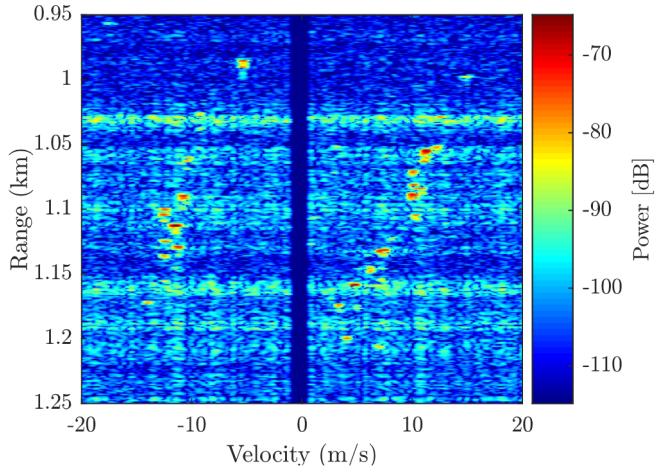


Fig. 6. Measured range-Doppler response from 2500 PRO-FM waveforms with moving spectral notches (using MF)

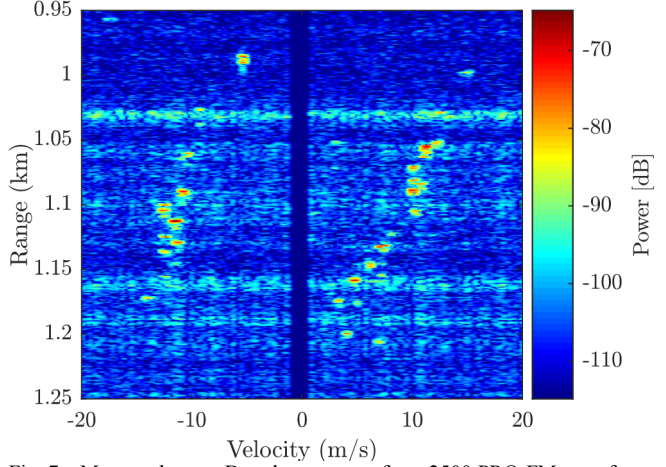


Fig. 7. Measured range-Doppler response from 2500 PRO-FM waveforms with moving spectral notches (using MMF)

C. Random notched FM waveforms with DeCCaF

Figures 8 and 9 show the MF and notched MMF range-Doppler responses, respectively, for the same set of notched waveforms when DeCCaF is applied using the borrowed clutter generated by the adjacent full-band waveforms. From a qualitative standpoint the MF DeCCaF result in Fig. 8 is rather similar to the previous MMF result of Fig. 7 (no DeCCaF). While not identical, the remaining streaks are similar, particularly the prominent one at a range of roughly 1.04 km that is believed to have been caused by the interaction between notch-induced nonstationarity and a clutter discrete at that range.

More interesting, however, is the response in Fig. 9 where both DeCCaF and notched MMFs have been applied. From a purely qualitative perspective this result is quite similar to what was originally obtained in Fig. 4 for matched filtering of full-band waveforms. In other words, this combination of approaches seems to have come rather close to completely compensating for degradation imposed by spectral notches that address dynamic RFI.

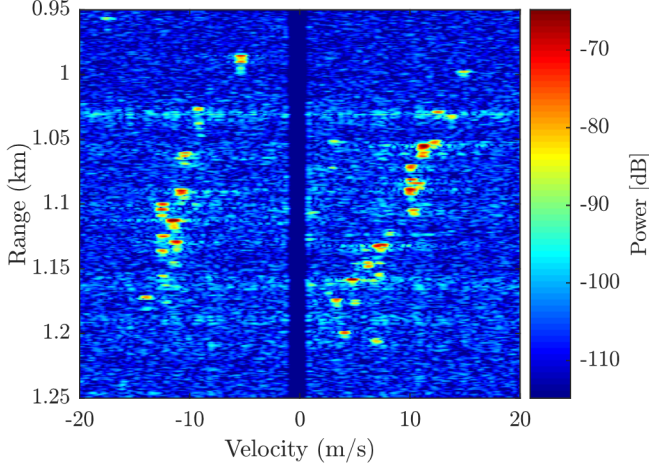


Fig. 8. Measured range-Doppler response from 2500 PRO-FM waveforms with moving spectral notches, applying interleaved & spectrally-filtered full-band responses for clutter filling (MF and DeCCaF)

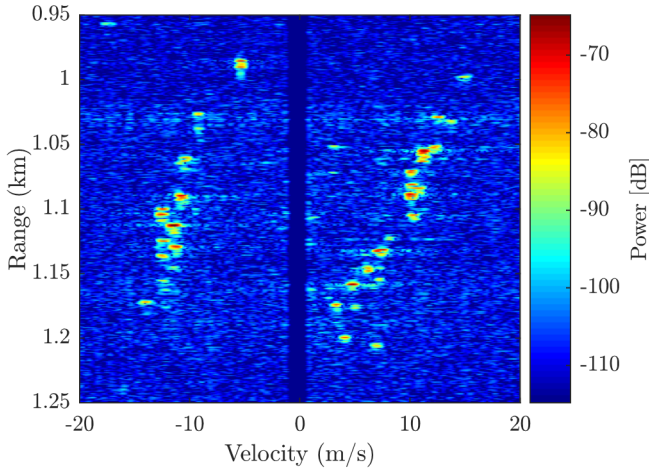


Fig. 9. Measured range-Doppler response from 2500 PRO-FM waveforms with moving spectral notches, applying interleaved & spectrally-filtered full-band responses for clutter filling (MMF and DeCCaF)

D. Random notched FM waveforms with DeCCaF, using notched pulses only

Having established the performance enhancement of DeCCaF when the borrowed clutter responses are taken from the separate (interleaved) set of full-band waveforms, now consider the impact of borrowing clutter from other notched pulses within the same CPI. Specifically, the BPF clutter is borrowed from the temporally nearest notched waveform that has a non-overlapping notch location relative to the pulse under consideration, as shown in Fig 10.

The resulting DeCCaF response of (6) therefore involves the re-use of clutter and noise from elsewhere in the CPI, as opposed to the statistically independent instantiations considered in the previous interleaved case, which would likely not be realistic. Consequently, some degradation in the degree of residual clutter compensation is expected.

Figures 11 and 12 show the MF and MMF range-Doppler responses, respectively, for this arrangement. Compared to Figs. 8 and 9, the residual clutter floor is slightly increased, though the overall performance improvement relative to Figs. 6 and 7 without DeCCaF is still quite clear.

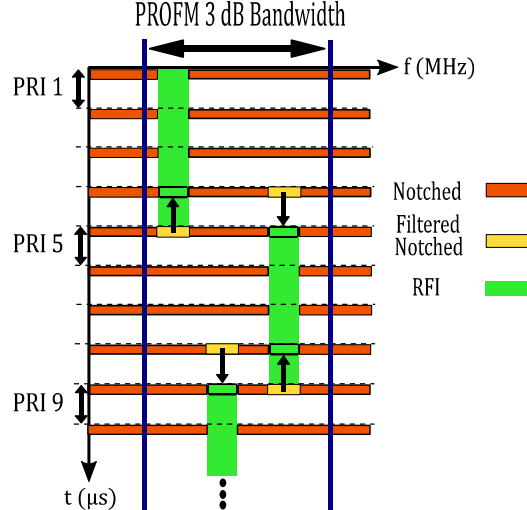


Fig. 10. Timing diagram of the waveform arrangement used to evaluate the operationally useful form of DeCCaF. The borrowed clutter is taken from temporally adjacent, spectrally non-overlapping notched responses.

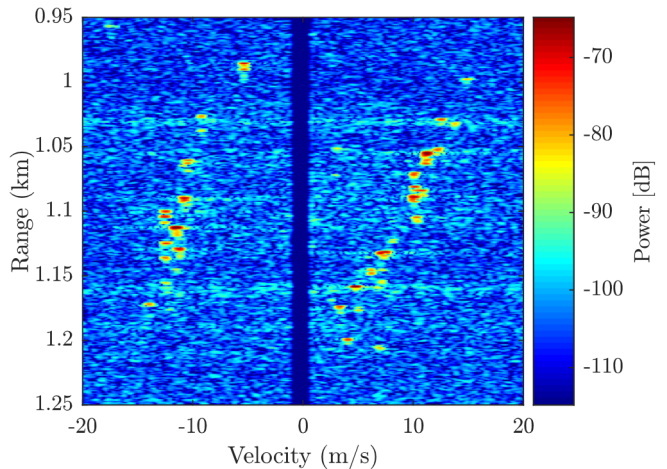


Fig. 11. Measured range-Doppler response from 2500 PRO-FM waveforms with moving spectral notches, applying adjacent spectrally-filtered notched waveform responses for clutter filling (MF and DeCCaF)

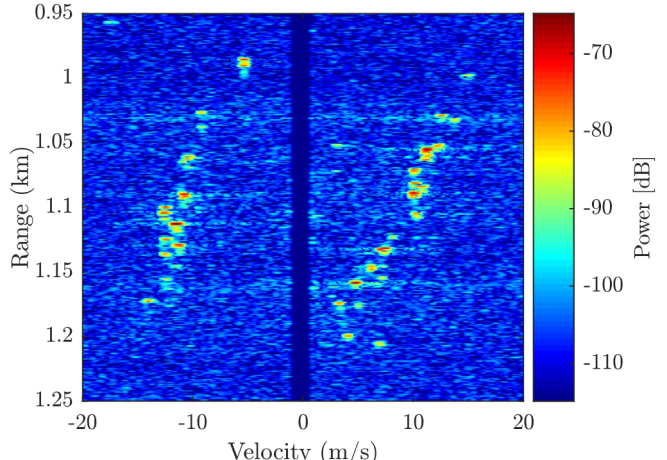


Fig. 12. Measured range-Doppler response from 2500 PRO-FM waveforms with moving spectral notches, applying adjacent spectrally-filtered notched waveform responses for clutter filling (MMF and DeCCaF)

Finally, for a different perspective on how DeCCaF is compensating for notch-induced clutter modulation, the root-mean-squared (RMS) average of the MMF range estimate power spectral densities (PSD) across the CPI in slow-time are examined for Case 1 (full-band), Case 2 (notched without clutter filling), and Case 4 (notched, clutter filling with other notched responses). As Fig. 13 illustrates, the PSD employing moving notches exhibits a noticeable deviation from the PSD when full-band waveforms are used. However, refilling the missing clutter response via DeCCaF returns the PSD quite closely to the full-band case.

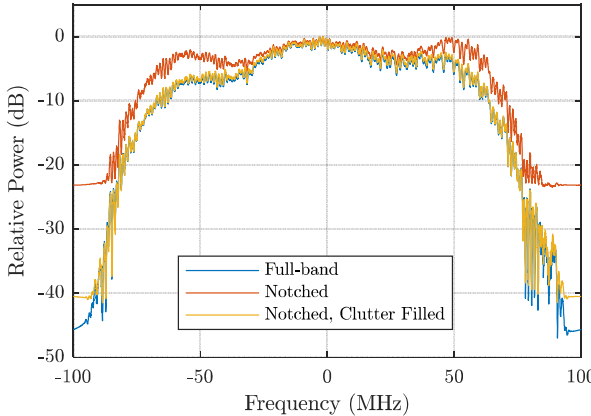


Fig. 13. RMS average of the MMF range estimate power spectral densities over the given CPI for Case 1 (full-band), Case 2 (notched without clutter filling), and Case 4 (notched, clutter filling with other notched responses).

VI. CONCLUSIONS

An ad hoc approach denoted as devoid clutter capture and filling (DeCCaF) has been proposed and demonstrated on measured data as a means to address the nonstationarity that arises when spectral notches must move during the CPI to combat dynamic RFI. When DeCCaF is combined with appropriately notched optimal mismatched filtering the result is nearly indistinguishable from the case in which no spectral notches are employed at all.

REFERENCES

- [1] H. Griffiths, et al, "Radar spectrum engineering and management: technical and regulatory Issues," *Proc. IEEE*, vol. 103, no. 1, pp. 85-102, Jan. 2015.
- [2] J.M. Peha, "Sharing spectrum through spectrum policy reform and cognitive radio," *Proc. IEEE*, vol. 97, no. 4, pp. 708-719, Apr. 2009.
- [3] M. Labib, V. Marojevic, A.F. Martone, J.H. Reed, A.I. Zaghloul, "Coexistence between communications and radar systems – a survey," *URSI Radio Science Bulletin*, vol. 2017, no. 362, pp. 74-82, Sept. 2017.
- [4] S.D. Blunt, E.S. Perrins, *Radar & Communication Spectrum Sharing*, SciTech Publishing, 2018.
- [5] M. López-Benítez, "Sensing-based spectrum awareness in cognitive radio: challenges and open research problems," *Int'l. Symp. Communication Systems, Networks & DSP*, Manchester, UK, July 2014.
- [6] A.F. Martone, "Cognitive radar demystified," *URSI Bulletin*, no. 350, pp. 10-22, Sept. 2014.
- [7] P. Stinco, M.S. Greco, F. Gini, "Spectrum sensing and sharing for cognitive radars," *IET Radar, Sonar & Navigation*, vol. 10, no. 3, pp. 595-602, Feb. 2016.
- [8] A. Farina, A. De Maio, S. Haykin, *The Impact of Cognition on Radar Technology*, SciTech Publishing, 2017.
- [9] A. Martone, K. Ranney, K. Sherbondy, K. Gallagher, S. Blunt, "Spectrum allocation for non-cooperative radar coexistence," *IEEE Trans. Aerospace & Electronic Systems*, vol. 54, no. 1, pp. 90-105, Feb. 2018.
- [10] B.H. Kirk, K.A. Gallagher, J.W. Owen, R.M. Narayanan, A.F. Martone, K.D. Sherbondy, "Cognitive software defined radar for time-varying RFI avoidance," *IEEE Radar Conf.*, Oklahoma City, OK, Apr. 2018.
- [11] B. Ravenscroft, J.W. Owen, J. Jakabosky, S.D. Blunt, A.F. Martone, K.D. Sherbondy, "Experimental demonstration and analysis of cognitive spectrum sensing and notching for radar," *IET Radar, Sonar & Navigation*, vol. 12, no. 12, pp. 1466-1475, Dec. 2018.
- [12] J. Jakabosky, S. D. Blunt, B. Himed, "Spectral-shape optimized FM noise radar for pulse agility," *IEEE Radar Conf.*, Philadelphia, PA, May 2016.
- [13] C.A. Mohr, S. D. Blunt, "Analytical spectrum representation for physical waveform optimization requiring extreme fidelity," *IEEE Radar Conf.*, Boston, MA, Apr. 2019.
- [14] B. Ravenscroft, S.D. Blunt, C. Allen, A. Martone and K. Sherbondy, "Analysis of spectral notching in FM noise radar using measured interference," *IET Intl. Conf. Radar Systems*, Belfast, UK, Oct. 2017.
- [15] B. Ravenscroft, J.W. Owen, S.D. Blunt, A.F. Martone, K.D. Sherbondy, "Optimal mismatched filtering to address clutter spread from intra-CPI variation of spectral notches," *IEEE Radar Conf.*, Boston, MA, Apr. 2019.
- [16] D. Henke, P. McCormick, S.D. Blunt, T. Higgins, "Practical aspects of optimal mismatch filtering and adaptive pulse compression for FM waveforms," *IEEE Radar Conf.*, Arlington, VA, May 2015.
- [17] S.D. Blunt, M.R. Cook, J. Stiles, "Embedding information into radar emissions via waveform implementation," *Intl. Waveform Diversity & Design Conf.*, Niagara Falls, Canada, Aug. 2010.
- [18] C. Sahin, J. Metcalf, S. Blunt, "Filter design to address range sidelobe modulation in transmit-encoded radar-embedded communications," *IEEE Radar Conf.*, Seattle, WA, May 2017.
- [19] A.C. O'Connor, J.M. Kantor, J. Jakabosky, "Filters that mitigate waveform modulation of radar clutter," *IET Radar, Sonar & Navigation*, vol. 11, no. 8, pp. 1188-1195, May 2017.
- [20] C.C. Jones, S.D. Blunt, "Mismatched complementary-on-receive filtering of diverse FM waveform subsets," *Intl. Radar Conf.*, Toulon, France, Sept. 2019.
- [21] A. Liu, Y. S. Lim, K. C. Teh and C. Gao, "Mismatched filter for transmit waveform with frequency notches," in *IET Radar, Sonar & Navigation*, vol. 12, no. 3, pp. 332-340, 3 2018.
- [22] K.M. Cuomo, J.E. Piou, J.T. Mayhan, "Ultrawide-band coherent processing," *IEEE Trans. Antennas & Propagation*, vol. 47, no. 6, pp. 1094-1107, June 1999.
- [23] J. Salzman, D. Akamine, R. Lefevre, J.C. Kirk, "Interrupted synthetic aperture radar (SAR)," *IEEE Aerospace & Electronic Systems Magazine*, vol. 17, no. 5, pp. 33-39, May 2002.